INFLUENCE OF PROCESSES ON THE SUN AND IN THE INTERPLANETARY MEDIUM ON THE SOLAR PROTON EVENT ON MARCH 30, 2022

© 2025 N.A. Vlasova[1,*], G.A. Bazilevskaya[2], E.A. Ginzburg[3], E.I. Daibog[2], Kalegaev[1,4], K.B. Kaportseva[1,4], Yu.I. Logachev[a], I.N. Myagkova[a]

[1]*Skobeltsyn Institute of Nuclear Physics, Moscow State University, Moscow, Russia*

[2]*Lebedev Physical Institute, Russian Academy of Sciences, Moscow, Russia*

[3]*Fedorov Institute of Applied Geophysics, Moscow, Russia*

[4]*Faculty of Physics of Lomonosov Moscow State University, Moscow, Russia*

**e-mail: nav19iv@gmail.com*

**e-mail: nav19iv@gmail.com*

Received March, 02 2024

Revised April, 01 2024

Accepted for publication July, 25 2024

The results of a comparative analysis of the solar proton event on 30.03.2022, which has an unusual time profile of solar proton fluxes, with previous and subsequent solar proton events: 28.03.2022 and 02.04.2022 are presented. Increases in energetic proton fluxes in interplanetary and near-Earth space are associated with sequential solar flares of X-ray classes M4.0, X1.3, and M3.9 and three halo-type coronal mass ejections. The work is based on experimental data obtained from spacecraft located in interplanetary space (ACE, WIND, STEREO A, DSCOVR), in a circular polar orbit at an altitude of 850 km (Meteor-M2), and in geostationary orbit (GOES-16, Electro-L2). An explanation is proposed for the peculiarities of the energetic proton flux profile in the solar proton event on 30.03.2022: protons accelerated in the flare on 30.03.2022 were partially shielded by an interplanetary coronal mass ejection, the source of which was explosive processes on the Sun on 28.03.2022; the late registration of maximum proton fluxes, simultaneous for particles of different energies, is due to the arrival of particle fluxes inside the interplanetary coronal mass ejection. The spatial distribution of solar protons in near-Earth orbit was similar to the distribution at the Lagrange point *L1* , but with a delay of ~50 min. *Keywords: solar proton event, solar flare, coronal mass ejection, solar wind, interplanetary magnetic field*

DOI: 10.31857/S00167940250103e3

1. INTRODUCTION

Solar proton events (SPEs) recorded in near-Earth space are the result of many physical processes occurring in the solar corona, in the interplanetary medium, and even in Earth's magnetosphere. Statistical patterns, typical and extreme characteristics of SPEs can be determined using SPE catalogs, which contain a multi-year homogeneous series of experimental data (for example, [Logachev et al., 2022]). But only the results of a specific event study depict the true picture of phenomena occurring on the Sun and in the interplanetary medium. Despite years of research, there is no unambiguous solution to the question of the source of energetic solar particles. After the discovery of solar cosmic rays, flares were considered their source [Meyer et al., 1956]. Results of coronal mass ejection (CME) studies led to the understanding that particle acceleration is also possible on shock waves preceding CMEs [Kahler et al., 1984; Reames, 1995]. Currently, it is assumed that solar energetic particles are accelerated both in the solar flare region and on shock waves associated with CMEs (for example, [Reames, 2013, 2017; Bazilevskaya, 2017; Klein and Dalla, 2017]). Acceleration on shock waves accompanying CMEs can occur both during the CME formation on the Sun and in the interplanetary medium (for example, [Reames, 2013; Bazilevskaya et al., 2023]). At the same time, a very small number of SPEs were observed that were associated only with CMEs without solar flares [Marqué et al., 2006]. Models of solar energetic particle propagation have been created, taking into account particle acceleration in the solar corona and in the interplanetary medium [Frassati et al., 2022; Zhang et al., 2023].

The main factor determining dynamic processes in the interplanetary medium is the interplanetary magnetic field [Parker, 1965]. Magnetic inhomogeneities frozen into the solar wind plasma affect the movement of solar energetic particles and cause modulation of their fluxes with characteristic times from several minutes to several days. In particular, magnetic structures of the solar wind can form particle traps, capturing them in closed regions of space.

The empirical "reflective model" assumes the capture and transfer of particles in semi-transparent magnetic traps formed by the force lines of the interplanetary magnetic field (IMF) extending from the Sun [Lyubimov, 1988; Lyubimov and Grigorenko, 2007]. In [Daibog et al., 2017], the existence of variations in Jovian electron fluxes near Earth is explained, in particular,

by the presence of electrons in magnetic traps shaped like closed magnetic structures that arise from the interaction of solar wind streams with different velocities (*Stream Interaction Region* , SIR). If streams with different velocities exist for a long time, rotating with the Sun, then Corotating Interaction Regions (CIR) emerge, which can influence the dynamics of solar energetic particles (for example, [Richardson, 2004; 2018]). In [Reames, 2013; 2023], regions of space behind the propagating shock front containing trapped particles are described. In [Vlasova et al., 2024], to explain the long-term observation of solar energetic proton fluxes in the heliosphere, the existence of a closed trap region formed by two interplanetary coronal mass ejections (ICMEs) and interaction regions between high-speed and slow solar wind flows has been proposed.

It is known that ICMEs affect the flow of solar energetic particles. Data from the Explorer-12 spacecraft revealed an increase in energetic particle fluxes, called *Energetic Storm Particles* , before a "plasma cloud" that caused a magnetic storm on Earth [Bryant et al., 1962]. The study concluded that these are solar protons trapped inside the plasma cloud. Results of the investigation of solar proton arrivals at the SOHO spacecraft, while it was inside a magnetic cloud, indicate that the magnetic field in the CME structure provides a "highway" for proton flux propagation [Torsti et al., 2004]. Using solar energetic particles as a tool to study the magnetic field topology of two magnetic clouds showed that in one case, based on particle reflection, the magnetic loop should be represented as a bottle connected to the Sun, while in the second case, reflection occurs from a magnetic mirror formed by the compression field behind the shock wave, indicating an open field line topology [Tan et al., 2014]. In [Shen et al., 2008], it was shown that the proton flux with energy ≥10 MeV in the event of 05.11.2011 was the largest in solar cycle 23 because the particles entered a structure consisting of a shock wave and a magnetic cloud. At the same time, for the event of 14.07.2000 (GLE 59), the profile of proton fluxes with energies from ~ 1 to ~ 100 MeV shows a two-stage rapid intensity decrease associated with the compression region and the magnetic cloud [Wu and Quin, 2020]. In [Cane et al., 1988], results are presented on the influence of the shock wave preceding the CME, which is in the path of particle propagation in the interplanetary medium, on the time profiles of solar protons depending on the heliographic longitude of their source. In [Kahler and Reames, 1991], it is concluded that magnetic clouds are almost transparent for solar particles (electrons with E = 0.2−2 MeV, protons with E = 22−27 MeV, ISEE-3 spacecraft) and the fields of magnetic clouds are not closed. In

[Masson et al., 2012], based on the results of GLE event studies using neutron monitor data, it is shown that the arrival time of the first high-energy particles on Earth is largely determined by the type of IMF in which the particles propagate. The initial arrival time corresponds to what is expected in the Parker model with slow solar wind and is significantly longer in heliospheric structures such as ICMEs. In [Kocharov et al., 2005], it is concluded that the CME structure, similar to a magnetic trap, significantly changes the intensity-time profile of high-energy particles observed at 1 AU. The particle flux decrease after the maximum occurs more slowly than when modeling with an Archimedean spiral magnetic field and can be approximated by an exponential function.

The purpose of this work is to explain the reasons for the formation of the complex temporal profile of solar energetic proton fluxes on March 30-31, 2022, which differs from the corresponding profiles in the previous and subsequent solar proton events on March 28, 2022, and April 1, 2022, based on the results of analysis of solar sources of energetic particles and high-speed solar wind streams, as well as conditions in the interplanetary medium in which solar protons propagated from the Sun to Earth's orbit.

2. SOURCES OF EXPERIMENTAL DATA

The study of temporal profiles of solar proton fluxes on March 28, 2022, March 30, 2022, and April 2, 2022, was performed based on experimental data obtained from spacecraft (SC) located in interplanetary space and in Earth's magnetosphere (Table 1).

TABLE 1

The STEREO A spacecraft during the study period (March 30, 2022) was located at a distance of 0.97 AU from the Sun, and the region on the Sun connected to the spacecraft by magnetic field lines at a solar wind speed of 400 km/s is approximately 35.3° ° east of the corresponding region for Earth [Gieseler et al., 2022; https://solar-mach.github.io/].

Electronic resources from which the necessary research information was obtained:

- on solar flares and coronal holes (https://www.solarmonitor.org/);
- on coronal mass ejections from the LASCO/C2 coronagraph on the SOHO spacecraft (https://cdaw.gsfc.nasa.gov/CME_list/);
- on the position of dimmings to determine the heliocoordinates of CMEs (https://www.sidc.be/solardemon/);

- on images of the Sun in various wavelengths from the SDO spacecraft (https://www.spaceweatherlive.com ; https://www.sidc.be/solardemon/);

- on synoptic maps of the Sun (https://gong.nso.edu/);

- on the arrival time of CME shock waves in near-Earth space (NES) (https://zenodo.org/record/7991430);

- on the results of modeling the arrival of ICMEs in near-Earth space by the solar wind and CME forecast service of the Euler Institute of St. Petersburg State University and LETI (https://solarwind.entroforce.ru/);

- on solar wind and interplanetary magnetic field from the ACE spacecraft and DSCOVR spacecraft (https://swx.sinp.msu.ru/);

- on solar energetic particle fluxes from STEREO A and WIND spacecraft (https://cdaweb.gsfc.nasa.gov/), from ACE spacecraft and GOES-16, Meteor-M2, Electro-L2 satellites (https://swx.sinp.msu.ru/).

Most of the figures in this article were created on the website of the Center for Operational Space Monitoring Data (CDOKM) of SINP MSU, which provides access to operational data from space experiments and models for operational forecasting of space weather phenomena. The CDOKM website in the "Space Weather" section (https://swx.sinp.msu.ru/) contains data necessary for evaluating and analyzing the radiation environment not only in near-Earth space but also in the interplanetary medium. The site also presents electronic interactive versions of catalogs of solar proton events for solar cycles 24 and 25 and links to printed versions of SPE catalogs for solar cycles 20-24 (https://swx.sinp.msu.ru/apps/sep_events_cat/index.php?gcm=1&lang=ru).

Advanced graphical applications enable comparative analysis of both experimental data and modeling results.

3. EXPERIMENTAL RESULTS

A distinctive feature of the discussed solar proton event of 30.03.2022 is that the time profiles of particle fluxes have a more complex form compared to the profiles of the preceding (28.03.2022) and subsequent (02.04.2022) events (Fig. 1 *b*). The SPEs of 28.03.2022, 30.03.2022, and 02.04.2022 are associated with solar flares of X-ray classes (Fig. 1 *a*) M4.0 (W09), X1.3 (W31), and M3.9 (W68), respectively (heliolongitude of the flare is indicated in

parentheses). The flares of 28.03.2022 and 30.03.2022 occurred in the same active region. All three flares were accompanied by halo-type CMEs. Conditions in the interplanetary medium during the propagation of particles from the three SPEs were different (Fig. 1 *c* , 1 *d*). Each event was accompanied by a high-speed solar wind stream. In the last ten days of March 2022, two coronal holes (CH) passed through the central meridian of the Sun: 22−24.03.2022 – a near-equatorial one of quite large area; 29−31.03.2022 – a mid-latitude one of small area. High-speed solar wind streams, through which the Earth passed on 27−28.03.2022 and 02.04.2022 (Fig. 1 *c*), could have these CHs as their sources, as the stream velocities were ~ 550 km/s, which corresponds to a propagation time from the Sun to the Earth of – ~ 3 days. On 28.03.2022, two flares of classes M4.0 and M1.0 occurred in the active region AR12975 located near the center of the solar disk, with a time difference of about 8 hours, accompanied by "halo" type coronal mass ejections. The SPE of 28.03.2022 is associated with the first flare; after the second flare, no additional increase in the solar proton flux was registered. The interaction of the two CMEs led to the formation of an ICME propagating toward Earth. The arrival of the shock wave associated with this ICME was recorded on 31.03.2022 at 01:44 UT at the L1 point and at 02:24 UT in Earth orbit (https://zenodo.org/record/7991430).

FIG. 1.

It can be seen that during the SEP on 03/30/2022, the strongest IMF was observed, as well as a prolonged large negative value of the *Bx* -component of the IMF (Fig. 1 *d*). Temporal profiles of solar proton fluxes, presented in Fig. 1 *b* , are constructed based on measurements inside the Earth's magnetosphere from the GOES-16 satellite. A similar shape of all three profiles of energetic proton fluxes was observed at the Lagrangian point *L1* on the ACE spacecraft (Fig. 2 *a*), and in the polar cap regions of Earth on open field lines of Earth's magnetic field on the Meteor-M2 satellite in the northern and southern polar caps (Fig. 2 *b*), and in geostationary orbit on closed field lines on the Electro-L2 satellite (Fig. 2 *c*). Consequently, it can be said that the features of particle flux profiles on 03/30/2022 are not related to the penetration of particles into Earth's magnetosphere.

FIG. 2.

For a more accurate assessment of the differences in the temporal profile of solar proton fluxes on 03/30-31/2022 from the profiles in the SEP events of 03/28/2022 and 04/02/2022, Fig. 3 shows, in a unified scale, the profiles of proton fluxes according to GOES-16 satellite data

during the first day after the solar flares associated with the SEP events. Several features of the profile on 03/30/2022 can be distinguished (Fig. 3 *b*):

FIG. 3.

beginning of increase in fluxes of particles with energy > 5 MeV and > 10 MeV occurs earlier than the time of increase in fluxes of more energetic particles (E > 100 MeV), which argues against their origin from a single source;

- the time interval between the flare onset and the arrival of particles with E > 100 MeV for the SEE on 03.30.2022 is 109 minutes, which is significantly longer than for the SEE on 03.28.2022 (47 min) and SEE on 04.02.2022 (46 min), and does not correlate with the distance between the flare longitude and the Earth's connection longitude;

- the time interval between the flare onset and the observation of maximum proton flux values with E >10 MeV for the SEE on 03.30.2022 (~ 12.6 hours) is substantially longer than for the SEE on 03.28.2022 (~ 4 hours) and SEE on 04.02.2022 (~ 3 hours); the time of maximum observation in the SEE on 03.28.2022 and 04.02.2022 depends on proton energy, while in the SEE on 03.30.2022, the maximum proton fluxes of different energies were observed simultaneously;

- the maximum proton flux, especially in the higher energy range, in the SEE on 03.30.2022 is significantly lower than in the other two events, despite the fact that the X-ray flare magnitude on 03.30.2022 is the highest: X1.3 compared to M4.0 and M3.9;

- the shape of the particle flux profile before the maximum differs significantly for the event on 03.30.2022.

FIG. 4.

Figure 4 shows the SEEs on 03.28.2022 and 03.30.2022 based on observations from the WIND spacecraft and STEREO A spacecraft, which at the end of March 2022 was located at a distance of 0.97 AU from the Sun and 33.5° ° east of Earth. The time profiles of solar proton fluxes measured at the L1 libration point *L1* on the WIND spacecraft and on STEREO A almost coincide on 03.28.2022. In the event on 03.30.2022, the profile from STEREO A data differs little from that of 03.28.2022, while at the WIND spacecraft at the point *L1* a significant difference is observed between the profiles of 03.28.2022 and 03.30.2022.

4. DISCUSSION

The complex temporal profile of solar energetic proton fluxes on 03.30-31.2022 may be due to the peculiarities of particle generation and acceleration processes on the Sun and propagation in the interplanetary medium.

4.1 Conditions on the Sun

An analysis of solar sources of particle fluxes and disturbed solar wind during the studied time period was conducted using images of the solar disk in ultraviolet light at times presumably corresponding to the observation of CMEs in the lower corona of the Sun (https://www.spaceweatherlive.com/), and images of CMEs in the coronagraph (https://www.sidc.be/cactus/catalog/LASCO/2_5_0/qkl/2022/03/). Additionally, difference images were studied (obtained by sequential subtraction of frames from the first frame for each observation) at a wavelength of 21.1 nm (https://www.sidc.be/solardemon/), the so-called "coronal dimmings" – darker areas in the image caused by density fluctuations in the solar corona (for example, [Reinard and Biesecker, 2008]). Coronal dimmings can be associated, among other things, with the ejection of CMEs from the corona. The analysis results showed that the location of dimmings corresponds to the location of flares and is consistent with the propagation direction of CMEs observed in the coronagraph. This indicates that the flares were indeed accompanied by the observed CMEs and the processes were localized approximately in the same region of the Sun, and also allows determining the temporal and spatial parameters of CME evolution in the early stages.

TABLE 2.

Table 2 presents parameters of solar flares, coronal mass ejections, active regions (AR) on the Sun, and calculated values obtained from solar images and the average solar wind speed during SEP observations.

During the early evolution of CMEs, they can affect the coronal propagation of solar protons (for example, [Zhang et al., 2023]). We compared the characteristics of the corresponding dimmings to check whether the differences in SEP events observed on 28.03.2022, 30.03.2022, and 02.04.2022 could be explained by differences in proton propagation in the solar corona. We estimated the time difference between the flare (according to X-ray data) and the beginning of CME expansion (according to difference images of the Sun). In the case of the SEP event on 30.03.2022, this is the shortest time: 9 minutes compared to 22 and 19 minutes. The parameters

of the three CMEs obtained from coronagraph data do not differ significantly (Table 2), although the CME on 30.03.2022 is slower and has the largest position angle. Based on the average solar wind velocity during the arrival of the first solar energetic protons in near-Earth space, we calculated the longitude of the region on the Sun connected with Earth by interplanetary magnetic field lines. The difference between the obtained longitude and the flare longitude corresponds to the angular distance of coronal proton propagation. For the SEP event on 30.03.2022, it is practically the smallest. The analysis results presented in Table 2 show that in all three cases, the difference between the source longitude and the geoeffective longitude cannot provide the observed difference in the time of SEP registration near Earth's orbit. Also, the CME velocities determined in the coronagraph do not indicate fundamental differences in the event of 30.03.2022 from the others. If we assume a coronal expansion velocity of ~ 1000 km/s, then the coronal propagation time from the point of disturbance initiation to the geoeffective longitude will be 8, 6, and 5 minutes for the three consecutive events considered. Thus, the features of the time profile of particle fluxes on 30.03.2022 were not related to the propagation of particles in the solar corona.

Analysis of synoptic maps of the Sun (https://gong.nso.edu/) showed that on 28.03.2022, the flare and the connection point with the STEREO A spacecraft were in a region of negative magnetic field, while the connection point with Earth (with the libration point *L1*) was in a region of positive field and separated from the flare by a polarity division line, but the patterns of temporal profiles of particle fluxes on the STEREO A spacecraft and at point *L1* coincide (Fig. 4).

FIG. 4.

In the event of 30.03.2022, the relative position of the flare, STEREO A spacecraft, and Earth changed little, while the profiles of the initial phase of proton flux increase according to STEREO A and WIND spacecraft data differ very significantly. Consequently, the polarity inversion line did not affect the coronal propagation of protons in the event of 30.03.2022. This conclusion is consistent with previously obtained research results indicating that heliospheric current sheet crossings do not affect the decay profile of solar proton fluxes with energies of 1-5 MeV [Kecskeméty et al., 2009]. The above research results on conditions and processes on the Sun during the three events under consideration do not provide an opportunity to significantly distinguish the SEP event of 30.03.2022.

4.2 Conditions in the interplanetary medium

Let us consider the possible influence of conditions in the interplanetary medium on the flux of solar protons propagating from the Sun to near-Earth space. On 28.03.2022, 2 CMEs were registered in AR 12975, with the second one, observed about 8 hours later, having higher velocity (Table 2) and acceleration: at 20Rs (Rs - solar radius) the first CME had zero velocity, while the second had 1300 km/s. The interaction of the two CMEs led to the formation of an ICME, whose shock wave reached the *L1* point on 31.03.2022 at 01:44 UT, and Earth at 02:24 UT (https://zenodo.org/record/7991430).

Fig.5.

Figure 5 shows the temporal structure of the ICME at point *L* 1 and proton fluxes at *L1* according to the ACE spacecraft data and in geostationary orbit according to GOES-16 satellite data. Vertical dashed lines correspond to features of the temporal profile of the ICME and solar proton fluxes. Line 1 shows the arrival time of the shock front at point *L1* , followed by a turbulent region (the section between lines 1 and 3 in this figure) with rapid changes in the IMF components, characteristic of the magnetic cloud sheath [Burlaga et al., 1981; Burlaga, 1988]. Inside this region, between lines 1 and 2, a stronger IMF was observed, which was accompanied by an increase in solar proton fluxes to maximum values according to ACE spacecraft data. The IMF structures before line 3, corresponding to the inner part of the turbulent region, were accompanied by a small local decrease in particle fluxes on the ACE spacecraft. Line 3 corresponds to the entry into the magnetic cloud, with characteristic properties [Burlaga et al., 1981; Burlaga, 1988; Pal et al., 2020; Vörös et al., 2021]: enhanced magnetic field, slow changes in its direction (signs of field vector rotation), practical absence of IMF fluctuations, low solar wind density, and low plasma temperature (not shown in the figure). At moment 4, in our opinion, exit from the magnetic cloud is observed, as the rate of change in the magnetic field direction significantly decreases (*Bx* - and *By* -components practically stop changing). The catalog (https://izw1.caltech.edu/ACE/ASC/DATA/level3/icmetable2.htm) provides only the duration of the entire ICME (12:00 UT 03/31/2022 - 12:00 UT 04/01/2022).

As shown in Fig. 5, there is a time shift of ~50 min between the time profiles of proton fluxes measured on the ACE spacecraft and on the GOES-16 satellite – the time required for the solar wind to travel 1.5 million km at the solar wind speed (~ 500 km/s), which is currently observed at the *L1* point (Fig. 5 *b*). The magnetic field structure within the ICME maintained an

almost constant spatial distribution of particle fluxes within it, which may indicate that protons with energies of at least 60 MeV propagate in space together with the ICME. This phenomenon requires further study. Thus, the features of the time profile of solar proton fluxes in the event of 30.03.2022 are explained by conditions in the interplanetary medium, in particular, the role of the ICME. It should be noted that this ICME passed the STEREO A spacecraft, on which no peculiarities in the time profile of proton fluxes were observed.

We can try to estimate the radial size of the heliospheric structure through which the Earth passes:

- the total radial size of the ICME (according to the catalog (https://izw1.caltech.edu/ACE/ASC/DATA/level3/icmetable2.htm) from 12:00 UT 31.03.2022 to 12:00 UT 01.04.2022) at an average solar wind speed of ~ 500 km/s is ~ 0.3 AU;

- the radial size of the magnetic cloud (between dashed lines 3 and 4 in Fig. 5) ~ 0.18 AU.

The estimate of the ICME dimensions on 31.03.2022 is consistent with previously obtained results: 0.2÷0.4 AU [Lepping et al., 1990].

Fig. 6.

Analysis of the dynamics of the energy spectrum parameter of proton fluxes, when approximated by a power function, $E^{-\gamma}$ makes it possible to more accurately describe the various parts of the complex and unusual temporal profile of the particle flux on 30.03.2022. Figure 6 shows 5-minute values of proton fluxes according to GOES-16 satellite data and the integral energy spectrum parameter of solar protons in the power representation ($E > 5$ MeV ÷ $E > 100$ MeV). To obtain the spectrum, the background was subtracted - the average proton fluxes before the studied events, in the interval from 00:00 UT 27.03.2022 to 11:35 UT 28.03.2022. The spectrum parameters obtained from 5-minute data were smoothed over 13 points. The square marks the beginning of the solar flare on 30.03.2022, vertical segments 1 and 2 mark the beginning of the increase in proton fluxes in channels with $E > 10$ MeV and $E > 60$ MeV, segment 3 marks the arrival of the shock front.

It can be seen that the beginning of the growth of low-energy particle fluxes was observed earlier than the beginning of the increase in high-energy particles. These particles, most likely from the previous increase, were accelerated by the approaching shock front, which at the time of the flare on 30.03.2022 was at a distance of ~0.2 AU from Earth. This front also led to a delay in the arrival of the first particles from the flare on 30.03.2022 at 17:21 UT. With the arrival on

30.03.2022 at ~19:05 UT of more energetic particles from the flare on 30.03.2022, the spectrum becomes harder, γ rapidly decreases. The profiles of particle fluxes with E > 60 MeV and E >100 MeV before the shock wave indicate their diffusional propagation. The increase in γ after the shock wave is associated with the arrival of particles inside the ICME. From ~06 UT 31.03.2022 until the beginning of 01.04.2022, an almost exponential decrease in the proton flux is observed with a characteristic time of ~8 hours. The spectrum parameter γ gradually increases. This can be interpreted as the convective transport of particles in the expanding heliospheric structure experiencing adiabatic cooling [Owens, 1979; Daibog et al., 2004; Kecskeméty et al., 2009].

The results presented in this work are not the first to observe the impact of ICME on the flow of solar energetic particles, but previously obtained results were rather contradictory (see Introduction). The time profiles of solar particles both presented and in the work [Cane et al., 1988], and in the later book [Reames, 2017] do not resemble the solar proton flux profile of 30.03.2022-01.04.2022. The reflection model of particle accumulation, transport, and propagation assumes the existence of magnetic structures containing semi-transparent barriers/mirrors [Lyubimov and Grigorenko, 2007]. In the event of 30.03.2022 in Fig. 5 *d* one can see the accumulation of particles behind the barrier (moment 3), which is formed by a strong magnetic field and an area with increased density and speed of the solar wind (Fig. 5 *b*-*c*).

In the works [Reames, 2013; 2023], "reservoirs" are discussed in detail - extensive regions of space behind the propagating shock front containing trapped particles. The reservoir is located between the shock front and the Sun. According to [Reames, 2023], particle trapping in the reservoir is the result of interaction between particles accelerated at the shock front with Alfvén and/or hydromagnetic wave activity accompanying the shock front. Inside the reservoir, particle fluxes are uniform, the reservoir size can be several astronomical units in radius and several dozen degrees in longitude. The boundaries of the reservoir may partially coincide with the boundaries of the magnetic cloud. The heliospheric structure of 31.03.2022 can also be considered as a reservoir into which particles enter, already accelerated during the explosive process on the Sun on 30.03.2022. Particles propagate in the interplanetary medium from the Sun to Earth within the ICME. Thus, it can be stated that there is a fairly large variety of approaches to explaining the participation of IMF structures and associated shock waves in the formation of the observed SEP proton profiles.

5. CONCLUSION

Based on the results of a comparative analysis of the solar proton event on 30.03.2022 (X1.3), which has a complex time profile of solar proton fluxes, with the previous and subsequent solar proton events: 28.03.2022 (M4.0) and 02.04.2022 (M3.9), a scenario for the development of the SPE on 30.03.2022 in near-Earth space is proposed:

28.03.2022 as a result of explosive processes on the Sun, two CMEs emerge. The later but faster CME catches up with the earlier one, and an ICME is formed.

At the moment of the solar flare onset at 17:21 UT on 30.03.2022, the shock front of the ICME was at a distance of ~ 0.2 AU from Earth.

The solar event on 30.03.2022 begins at 17:21 UT in the same active region from which the two CMEs originated, and after a few minutes, protons reach the ICME, where the magnetic field strength reaches ~ 20 nT.

The ICME impedes the propagation of solar protons to Earth.

The spatial distribution of proton fluxes inside the ICME was similar at point *L1* and at Earth, but with a time delay of ~50 min.

The structure of the magnetic field inside the ICME maintained an almost constant spatial distribution of particle fluxes within it, which may indicate that protons with energies of at least 60 MeV propagate in space together with the ICME.

ACKNOWLEDGMENTS

We thank all researchers who provide their data on proton fluxes and solar wind parameters via the Internet. Experimental data were obtained from NASA's Goddard Space Flight Center: solar wind and interplanetary magnetic field data from OMNIWeb: High Resolution OMNI (http://omniweb.gsfc.nasa.gov/form/omni_min.html); solar proton flux data from CDAWeb: the Coordinated Data Analysis Web (https://cdaweb.gsfc.nasa.gov/). Information on solar flares and coronal mass ejections was obtained from Coordinated Data Analysis Workshops (CDAW) (https://cdaw.gsfc.nasa.gov), SOHO LASCO CME CATALOG (https://cdaw.gsfc.nasa.gov/CME_list/). CME shock arrival times were obtained from the website (https://zenodo.org/record/7991430)

We thank the staff of the solar wind forecast service (Euler IMI SPbSU, LETI) (https://solarwind.entroforce.ru/) who specifically visualized the situation in the heliosphere for March 28, 2022−April 03, 2022 at our request.

FUNDING

The research was carried out within the scientific program of the National Center for Physics and Mathematics (project "Nuclear and Radiation Physics").

REFERENCES

−*Bazilevskaya G.A., Daibog E.I., Logachev Yu.I.* Isolated solar cosmic ray events caused by the arrival of fast storm particles (ESP) // Geomagnetism and Aeronomy. V. 63. No. 4. P. 503−510. 2023 https://doi.org/10.31857/S0016794023600254

− *Daibog E.I., Logachev Yu.I., Keiler S., Kecskemety K.* Series of solar events with identical declines as a tool for identifying quasi-stationary states of interplanetary space // Cosmic Research. V. 42. No. 4. P. 376–383. 2004

−*Daibog E.I., Kecskemety K., Lazutin L.L., Logachev Yu.I., Surova G.M.* 27-day periodicity of Jovian electron fluxes in Earth's orbit // Astronomical Journal. V. 94. No. 12. P. 1062–1070. 2017. https://doi.org/10.7868/S0004629917120027

−*Logachev Yu.I., Bazilevskaya G.A., Vlasova N.A., E.A. Ginzburg, E.I. Daibog, V.N. Ishkov, L.L. Lazutin, M.D. Nguyen, G.M. Surova, O.S. Yakovchuk* Catalog of solar proton events of the 24th solar activity cycle (2009−2019). Moscow: WDC, 970 p. 2022. https://doi.org/10.2205/ESDB-SAD-008

− *Lyubimov G.P.* Reflection model of SCR movement in loop traps // Astronomical Circular of the USSR Academy of Sciences. No. 1531. P. 19−20. 1988

−*Lyubimov G.P., Grigorenko E.E.* On the reflection model of solar cosmic rays // Cosmic Research. V. 45. No. 1. P. 12–19. 2007

−*Parker E.N.* Dynamic processes in the interplanetary medium / Ed. by L.I. Dorman. M.: MIR, 1965

−*Bazilevskaya G.A.* Once again about origin of the solar cosmic rays // Journal of Physics: Conf. Series. V. 798. P. 012034. 2017. https://iopscience.iop.org/article/10.1088/1742-6596/798/1/012034/pdf

−*Bryant D.A., Cline T.L., Desai U.D., McDonald F.B.* Explorer 12 observations of solar cosmic rays and energetic storm particles after the solar flare of September 28, 1961 // J. Geophys. Res. V. 67. N 13. P. 4983–5000. 1962. https://doi.org/10.1029/JZ067i013p04983

−*Burlaga L., Sittler E., Mariani F., Schwenn R.* Magnetic Loop Behind an Interplanetary Shock: Voyager, Helios, and IMP 8 Observations // J. Geophys. Res. V. 86. N A8. P. 6673–6684. 1981. https://doi.org/10.1029/JA086iA08p06673

−*Burlaga L.F.* Magnetic clouds and force-free fields with constant alpha // J. Geophys. Res., Space Physics. V. 93. N A7. P. 7217−7224. 1988. https://doi.org/10.1029/JA093iA07p07217

−*Cane H.V., Reames D.V., von Rosenvinge T.T.* The role of interplanetary shocks in the longitude distribution of solar energetic particles // J. Geophys. Res. V. 93. N A9. P. 9555−9567. 1988. https://doi.org/10.1029/JA093iA09p09555

−*Frassati F., Laurenza M., Bemporad A., West M.J., Mancuso S., Susino R., Alberti T., Romano P.* Acceleration of Solar Energetic Particles through CME-driven Shock and Streamer Interaction // Astrophysical Journal. V. 926. N 2. P. 227−246. 2022. https://doi.org/10.3847/1538-4357/ac460e

−*Gieseler J., Dresing N., Palmroos C. et al.* Solar-MACH: An open-source tool to analyze solar magnetic connection configurations // Front. Astronomy Space Sci. V. 9. 2022. https://www.frontiersin.org/journals/astronomy-and-space-sciences/articles/10.3389/fspas.2022.1058810/full

−*Kahler, S.W., Sheeley Jr., N.R., Howard, R.A., Koomen, M.J., Michels, D.J., McGuire, R.E., von Rosenvinge, T.T., Reames, D.V.* Associations between coronal mass ejections and solar energetic proton events // J. Geophys. Res. V. 89. N A11. P. 9683−9693. 1984. https://doi.org/10.1029/JA089iA11p09683

−*Kahler S.W., Reames D.V.* Probing the Magnetic Topologies of Magnetic Clouds by Means of Solar Energetic Particles // J. Geophys. Res. V. 96, N. A6. P. 9419−9424. 1991. https://doi.org/10.1029/91JA00659

−*Kecskeméty K., Daibog E.I., Logachev Y.I., Kóta J.* The decay phase of solar energetic particle events // J. Geophys. Res. V. 114. N A6. 2009. https://agupubs.onlinelibrary.wiley.com/doi/pdf/10.1029/2008JA013730
−*Klein K.* -L *., Dalla S.* Acceleration and Propagation of Solar Energetic Particles // Space Sci. Rev. V. 212. P. 1107–1136. 2017. https://link.springer.com/article/10.1007/s11214-017-0382-4
−*Kocharov L., Kovaltsov G.A., Torsti J. Huttunen-Heikinmaa K.* Modeling the solar energetic particle events in closed structures of interplanetary magnetic field // J. Geophys. Res. V. 110. N A12. 2005. https://doi.org/10.1029/2005JA011082
−*Lepping R.* P., *Jones J.A., Burlaga L.F.* Magnetic Field Structure of Interplanetary Magnetic Clouds at 1 AU // J. Geophys. Res. V. 95. N A8. P. 11957−11965. 1990. https://doi.org/10.1029/JA095iA08p11957
−*Marqué C., Posner A., Klein K.L.* Solar energetic particles and radio-silent fast coronal mass ejections // Astrophys. J. V. 642. P. 1222–1235. 2006. https://iopscience.iop.org/article/10.1086/501157
−*Masson S., Démoulin P., Dasso S., Klein K.-L.* The interplanetary magnetic structure that guides solar relativistic particles // Astron. Astrophys. V. 538. N A32. 2012. https://doi.org/10.1051/0004-6361/201118145
−*Meyer P., Parker E.N., Simson J.A.* Solar Cosmic Rays of February, 1956 and Their Propagation through Interplanetary Space // Phys. Rev. V. 104. N 3. P. 768-783. 1956. https://journals.aps.org/pr/pdf/10.1103/PhysRev.104.768?casa_token=_yHvEAClLcEAAAAA%3AN2b4irIb6lbxj2NRvyjazm_9GMXbDKcHv9Y_ecZcJZzI_q0ZDfqSlQOwNxV7QCcsWNn_7OfaXp2VqmgB
−*Owens A. J.* Interplanetary diffusion of solar cosmic rays—A new approximate analytic solution // J. Geophys. Res. V. 84. N A8. P. 4451 – 4456. 1979. https://doi.org/10.1029/JA084iA08p04451
−*Pal S., Dash S., Nandy D.* Flux erosion of magnetic clouds by reconnection with the Sun's open flux // Geophys. Res. Lett. V. 47. N 8. e2019GL086372. 2020. https://doi.org/10.1029/2019GL086372
−*Reames D.V.* Solar energetic particles: A paradigm shift // Rev. Geophys . V. 33. S1. P. 585−589. 1995. https://doi.org/10.1029/95RG00188

−*Reames D.V.* The two sources of solar energetic particles // Space Science Reviews. 2013. V. 175. P. 53–92. https://doi.org/10.1007/s11214-013-9958-9
−*Reames D.V.* Solar Energetic Particles. A Modern Primer on Understanding Sources, Acceleration and Propagation / Part of the book series: Lecture Notes in Physics (LNP, volume 932) 2017
−*Reames D.V.* How Do Shock Waves Define the Space-Time Structure of Gradual Solar Energetic Particle Events? // Space Science Reviews. 2023. V. 219. A14. https://doi.org/10.1007/s11214-023-00959-x
−*Reinard A.A., Biesecker D.A.* Coronal mass ejection associated coronal dimmings // Astrophys. J. V. 674. P. 576−585. 2008. https://iopscience.iop.org/article/10.1086/525269
−*Richardson I.G.* Energetic particles and corotating interaction regions in the solar wind // Space Science Reviews. V. 111. P. 267–376. 2004. https://doi.org/10.1023/B:SPAC.0000032689.52830.3e
−*Richardson I.G.* Solar wind stream interaction regions throughout the heliosphere // Living Reviews in Solar Phys. V. 15. A1. 2018. https://doi.org/10.1007/s41116-017-0011-z
−*Shen C., Wang Y., Ye P., Wang S.* Enhancement of Solar Energetic Particles During a Shock – Magnetic Cloud Interacting Complex Structure // Solar Phys. V. 252. P. 409–418. 2008. https://link.springer.com/article/10.1007/s11207-008-9268-7
−*Tan L.C., Malandraki O.E., Reames D.V., Ng C.K., Wang L., Dorrian G.* Use of incident and reflected solar particle beams to trace the topology of magnetic clouds // Astrophys. J. V. 750. N 2. P. 146−167. 2012. https://iopscience.iop.org/article/10.1088/0004-637X/750/2/146/meta
−*Torsti J., Riihonen E., Kocharov L.* The 1998 may 2–3 magnetic cloud: an interplanetary "highway" for solar energetic particles observed with SOHO/ERNE // Astrophys. J. V. 600. P. L83–L86. 2004. https://iopscience.iop.org/article/10.1086/381575
−*Vlasova N.A., Bazilevskaya G.A., Ginzburg E.A., Daibog E.I., Kalegaev V.V., Kaportseva K.B., Logachev Yu I., Myagkova I.N.* Solar Energetic Proton Fluxes in Near-Earth Space on March 13–23, 2023 // Cosmic Res. V. 62. N 2. C. 197−209. 2024. https://link.springer.com/article/10.1134/S0010952523600282
−*Vörös Z., Varsani, A., Yordanova, E., Sasunov, Y. L., Roberts, O. W., Kis, Á., Nakamura R., Narita Y.* Magnetic reconnection within the boundary layer of a magnetic cloud in the solar

wind // Journal of Geophysical Research: Space Physics. V. 126. N 9. e2021JA029415. 2021. https://doi.org/10.1029/2021JA029415

−*Wu S.-S., Qin G.* Magnetic Cloud and Sheath in the Ground-level Enhancement Event of 2000 July 14. I. Effects on the Solar Energetic Particles // Astrophys. J. V. 904. N 2. P. 151−159. 2020. https://doi.org/10.3847/1538-4357/abc0f2

−*Zhang M., Cheng L., Zhang J., Riley P., Kwon R.Y., Lario D., Balmaceda L., Pogorelov N.V.* A Data-driven, Physics-based Transport Model of Solar Energetic Particles Accelerated by Coronal Mass Ejection Shocks Propagating through the Solar Coronal and Heliospheric Magnetic Fields // Astrophys. J.: Supplement Series. V. 266. N 2. P. 35−54. 2023. https://doi.org/10.3847/1538-4365/accb8e

Table 1. Information sources on solar energetic proton fluxes and solar wind parameters and interplanetary magnetic field

Spacecraft	**Orbit**	**Proton energy, MeV**
STEREO A	Heliocentric orbit, close to Earth's orbit;	40−60
ACE	Lagrange point *L1* – 1.5 million km from Earth towards the Sun	>10 >30
WIND	Lagrange point *L1* – 1.5 million km from Earth towards the Sun	28−72
DSCOVR	Lagrange point *L1* – 1.5 million km from Earth towards the Sun	–
Meteor-M2	Circular, sun-synchronous, morning Inclination 98.8 , ορβιταλ περιοδ 101.4 μιν , orbital period 101.4 min.	10−160
GOES-16	Geostationary orbit: altitude ~ 36000 km; inclination ~ 0 ° ; longitude – 75.2 °W	> 5 > 10 > 30 > 60 > 100 > 500
Elektro-L2	Geostationary orbit: altitude ~ 36000 km; inclination ~ 0 ° ; longitude – 14.5 °W	9−20 20−40

Table 2. Parameters of solar flares, coronal mass ejections, active regions (AR) on the Sun and calculated values

Flares: date, start time (UT)	**28.03.2022 10:58**	**28.03.2022 19:08**	**30.03.2022 17:21**	**02.04.2022 12:56**
Flare coordinates, magnitude, AR	N12W09 M4.0 12975	N14W07 M1.0 12975	N13W31 X1.3 12975	N12W68 M3.9 12976
CME data *	N14W04 11:20 22 min	N14W12	N13W32 17:30 9 min	N15W69 13:15 19 min
CME: time of appearance in the coronagraph field of view (UT)	12:00	20:24	18:00	13:36
CME: speed and opening parameters**	702 km/s 360 ° 127 °	905 km/s 360 ° 299 °	641 km/s 360 ° 298 °	1433 km/s 360 ° 263 °
Vsw W φ Δ φ ***	520 km/s W43 34 °	– – –	400 km/s W58 27 °	550 km/s W42 -26 °
CME: Co	1000 km/s 8 min	– –	1000 km/s 6 min	1000 km/s 5 min
Arrival time of protons with $E > 100$ MeV (UT), ΔT from flare	11:45 47 min	– –	19:10 109 min	13:40 46 min

Note: * CME coordinates (dimming), start time of CME expansion in the solar corona (UT) and ΔT from flare onset to CME expansion.

** CME speed according to coronagraph, angular opening (angular width) of CME near the Sun, position angle of the fastest segment of the CME leading edge - MPA (*measurement position angle*).

*** Solar wind and associated longitude of the field line from Earth (W φ) and Δ φ between it and the flare longitude.

Figure captions

Fig. 1. Time profiles for 27.03.2022−05.04.2022: (*a*) − solar X-ray flux density with wavelength 0.1−0.8 nm and (*b*) − solar proton fluxes according to GOES-16 satellite data, (*c*) − solar wind speed and density and (*d*) − modulus and *Bx* -component of IMF (*d*) − according to DSCOVR spacecraft data.

Fig. 2 . Time profiles of solar proton fluxes 27.03.2022−05.04.2022: (*a*) − with E>10 MeV and E>30 MeV according to ACE spacecraft data; (*b*) − with E=10-160 MeV according to Meteor-M2 satellite data; (*c*) − with E=9−20 MeV and E=20−40 MeV according to Elektro-L2 satellite data.

Fig. 3. Time profiles of proton fluxes according to GOES-16 satellite data: (*a*) − from 11:00 UT 28.03.2022 to 11:00 UT 29.03.2022, (*b*) − from 17:00 UT 30.03.2022 to 17:00 UT 31.03.2022, (*c*) − from 13:00 UT 02.04.2022 to 13:00 UT 03.04.2022.

Fig. 4. (*a*) − Time profiles of proton fluxes with E=28−72 MeV according to WIND spacecraft data and with *E* =40−60 MeV STEREO A spacecraft from 27.03.2022 to 01.04.2022. (*b*) − Schematic location of STEREO A spacecraft and Earth on 30.03.2022. (https://solar-mach.github.io/)

Fig. 5. Time profiles from 16:00 UT 30.03.2022 to 14:00 UT 01.04.2022: (*a)*− solar wind speed and density according to DSCOVR spacecraft data; (*b*) − modulus *B* and *Bx* and (*c*) − *By and иBz components* of IMF according to DSCOVR spacecraft data; solar proton fluxes with energy >10 and >30 MeV according to (*d*) − ACE spacecraft and (*e*) GOES-16 satellite

Fig. 6 . Time profiles of the power-law spectral index of proton fluxes (upper curve) and proton fluxes with E>10, 60, and 100 MeV according to GOES-16 satellite data for 30−31.03.2022: *1* – beginning of the increase in proton flux >10 MeV, *2*− >60 MeV, *3* – arrival of the shock front.

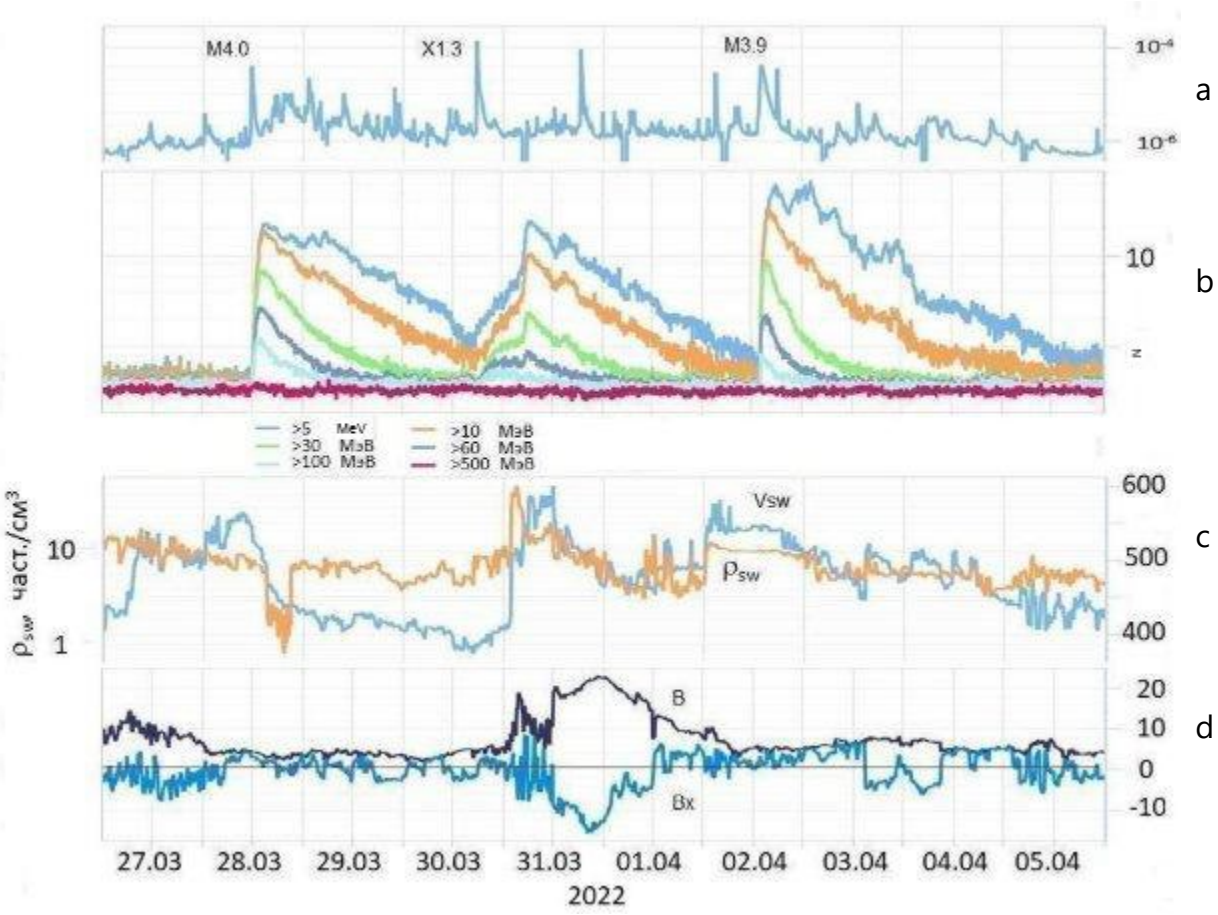
M4.0
X1.3
M3.9
a
b
>5 MeV
>30 МэВ
>100 МэВ
>10 МэВ
>60 МэВ
>500 МэВ
Vsw
ρ_{sw}
ρ_{sw} част./см^3
c
B
Bx
d
27.03
28.03
29.03
30.03
31.03
01.04
02.04
03.04
04.04
05.04
2022

Fig. 1.

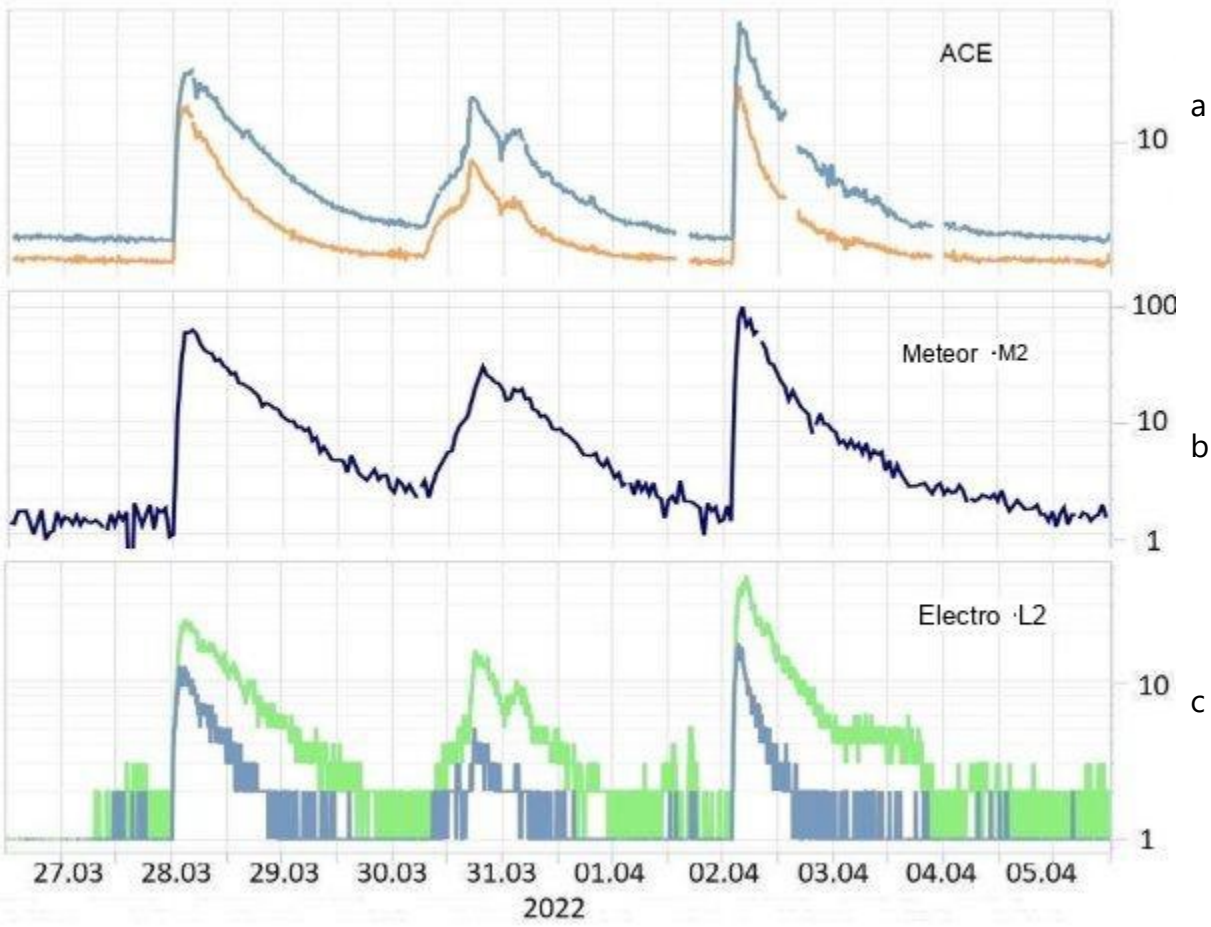
ACE
10
a
100
Meteor ·M2
10
1
b
Electro ·L2
10
1
c
27.03
28.03
29.03
30.03
31.03
01.04
02.04
03.04
04.04
05.04
2022

Fig. 2.

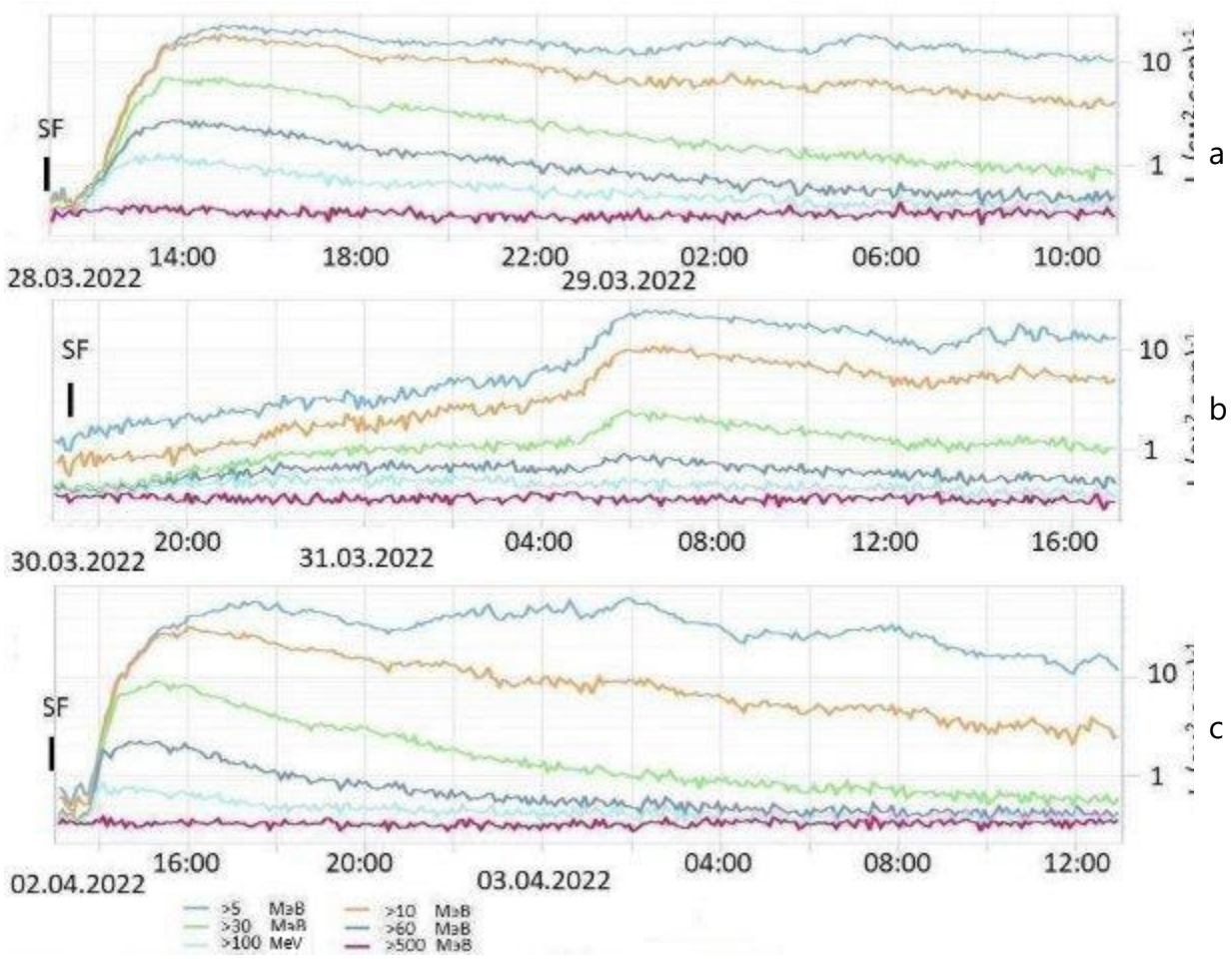
SF
10
1
a
14:00
18:00
22:00
02:00
06:00
10:00
28.03.2022
29.03.2022
SF
10
1
b
20:00
04:00
08:00
12:00
16:00
30.03.2022
31.03.2022
SF
10
1
c
16:00
20:00
04:00
08:00
12:00
02.04.2022
03.04.2022
>5 МэВ
>30 МэВ
>100 MeV
>10 МэВ
>60 МэВ
>500 МэВ

Fig. 3.

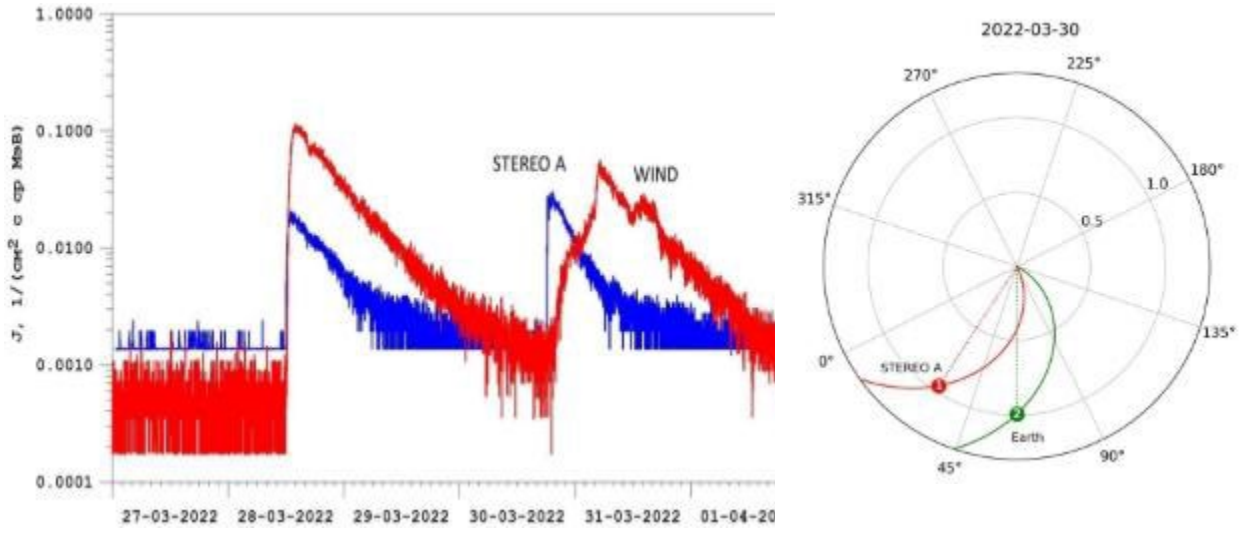
1.0000
0.1000
0.0100
0.0010
0.0001
J, 1/(cm² o cp MeB)
STEREO A
WIND
27-03-2022
28-03-2022
29-03-2022
30-03-2022
31-03-2022
01-04-20
2022-03-30
270°
225°
180°
315°
1.0
0.5
135°
0°
STEREO A
Earth
45°
90°

a *b*

Fig. 4.

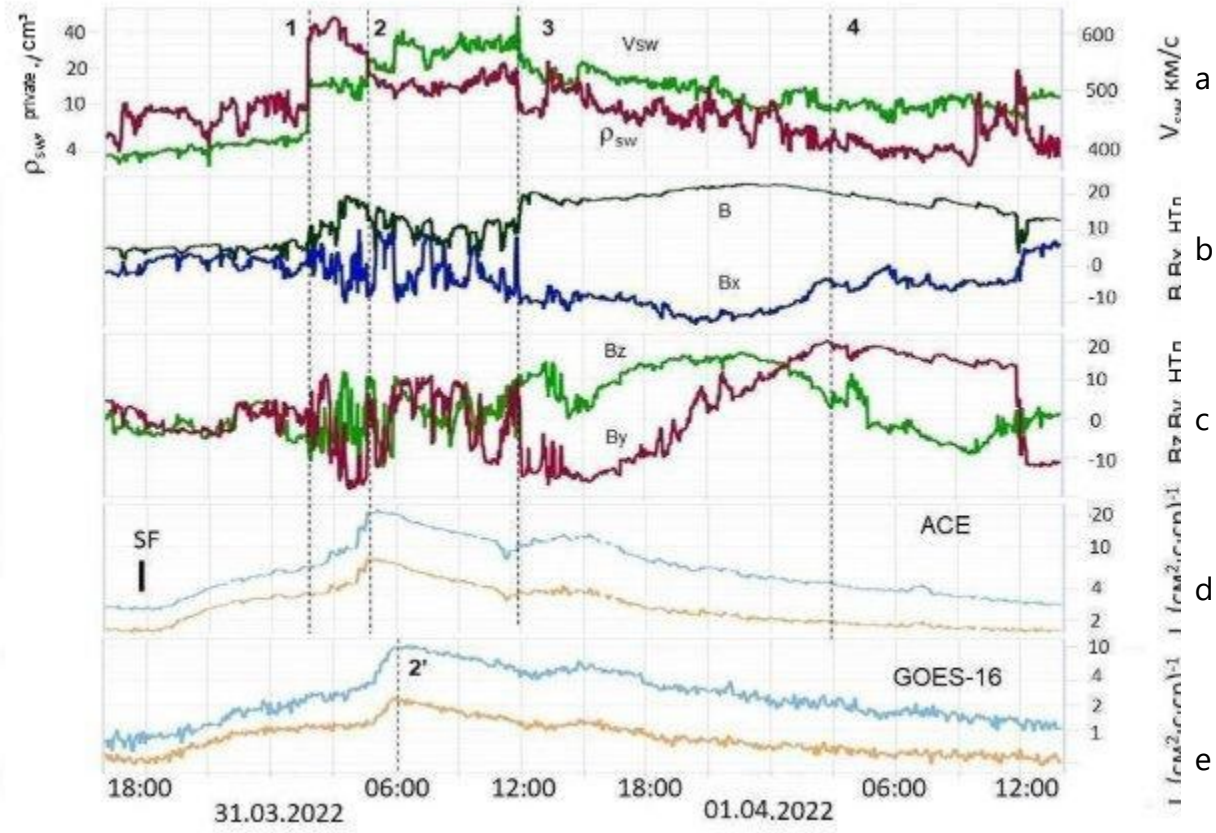
1
2
3
4
Vsw
ρsw
B
Bx
Bz
By
SF
ACE
2'
GOES-16
18:00
06:00
12:00
18:00
06:00
12:00
31.03.2022
01.04.2022
a
b
c
d
e

Fig. 5.

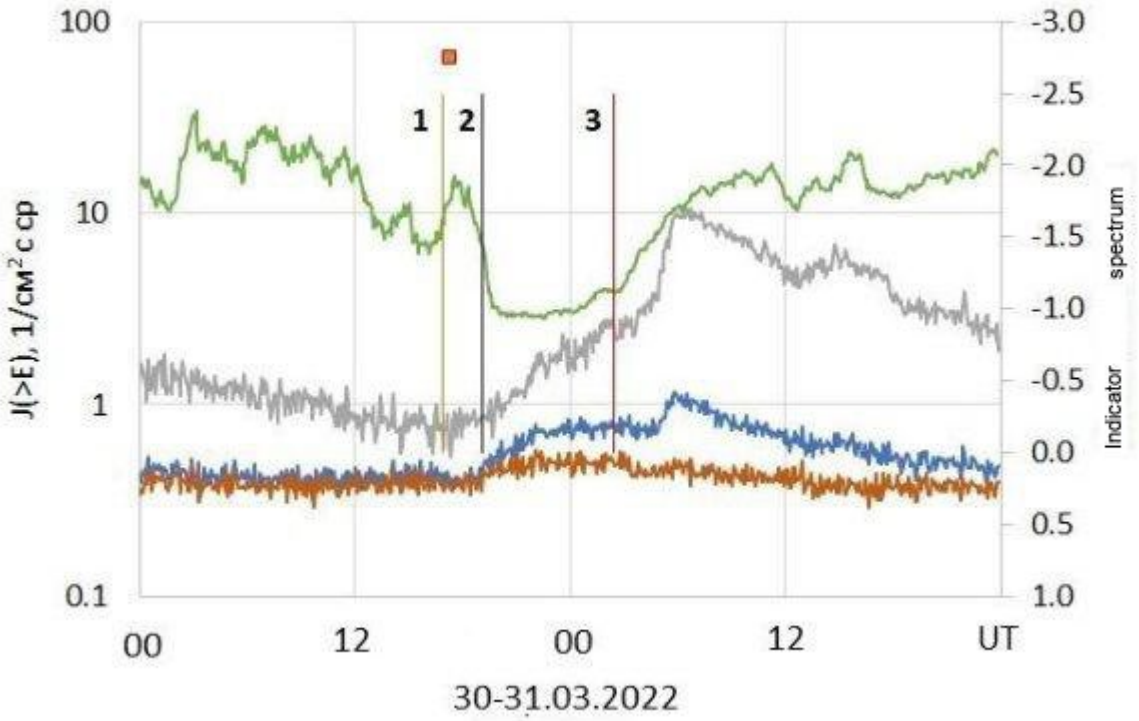
100
10
1
0.1
J(>E), 1/см² с ср
-3.0
-2.5
-2.0
-1.5
-1.0
-0.5
0.0
0.5
1.0
Indicator spectrum
1
2
3
00
12
00
12
UT
30-31.03.2022

Fig. 6.